

Mediated Spatiotemporal Registration of Cardiac DCE-MRI and Coronary MR Angiography

Constantine Zakkaroff¹, Derek Magee¹, Aleksandra Radjenovic², Roger Boyle¹

¹School of Computing, University of Leeds, Leeds, UK

²School of Medicine, University of Leeds, Leeds, UK

{mnkz, D.R.Magee, A.Radjenovic, R.D.Boyle}@leeds.ac.uk

Abstract. Patient-specific correlation of perfusion defects to coronary arteries which are responsible for blood supply in the affected territories has the potential to improve accuracy of diagnosis and intervention planning. The correlation of coronary arteries and perfusion defects can be established through registration of 3D angiography and 2D perfusion datasets. However, cardiac cycle phase mismatch between angiography and perfusion datasets causes the vast variation of the myocardium shape in these datasets and precludes the use of the standard methods for 2D/3D registration. Research published to date does not provide a reliable method of registering 2D perfusion and 3D angiography datasets. This paper presents an approach for non-rigid registration of 2D perfusion and 3D angiography data; the solution to the registration problem relies on the use of the 4D (3D + time) cine series to mediate non-rigid registration of perfusion and angiography datasets. The approach is evaluated on clinical data and its performance is compared with previously suggested methods for perfusion and angiography registration. The evaluation results show the utility of the presented method in the context of perfusion analysis while highlighting its applicability to other areas of cardiac image analysis.

Keywords: DCE-MRI, myocardial perfusion, MR angiography, slice-to-volume registration, mediated registration, spatiotemporal registration.

1 Introduction

Cardiovascular Magnetic Resonance (CMR) imaging provides in a single test the most comprehensive diagnostic information compared to other standard tests for Coronary Heart Disease (CHD) diagnosis; it allows for the assessment of ventricular function, tissue viability, coronary anatomy and myocardial perfusion in a single examination [1, 2]. In CMR imaging myocardial perfusion is assessed through Dynamic Contrast-Enhanced Magnetic Resonance Imaging (DCE-MRI) protocol; DCE-MRI is the most promising technique for non-invasive assessment of myocardial perfusion without the exposure to ionizing radiation [2]. 2D DCE-MRI time series show the quality of perfusion of the myocardium by imaging the passage of contrast agent through the heart. One of the goals of perfusion analysis is to

establish a reliable correlation between perfusion defects and coronary arteries responsible for the defects; this correlation is crucial for successful management of patients' treatment. There are two dominant approaches to perfusion analysis; one approach relies on pixel-by-pixel perfusion curves for the whole series; the other approach summarizes perfusion defects on a generic population-based bull's eye plot of coronary supply territories introduced by the American Heart Association [3]. In spite of the wide-spread use of the latter method it is unable to take into account clinically-important variability in coronary anatomy [4]. The accuracy of diagnosis and revascularization planning can be improved by correlating perfusion defects to the arteries responsible for blood supply in the affected areas of the myocardium in a patient-specific model. Registration of DCE-MRI and coronary Magnetic Resonance Angiography (MRA) datasets has the potential to provide the solution for patient-specific mapping of perfusion defects to coronary supply territories. However the standard methods of rigid and non-rigid registration are not applicable in this context because of the cardiac phase mismatch between DCI-MRI and MRA datasets. Myocardium shape variation across the heart cycle precludes the use of rigid slice-to-volume registration, while the difficulties associated with weak perspective in non-rigid slice-to-volume registration impede the use of the standard non-rigid techniques.

In this work we present an approach for mediated spatiotemporal registration designed to overcome the difficulties associated with perfusion and angiography registration. The method is based on the use of a non-rigid transform obtained from the analysis of temporal series (4D MR cine datasets). A non-rigid transform spanning the phases from angiography to perfusion is derived from the 4D cine; this transform is used as the spatiotemporal registration mediator in the process of correlating perfusion defects with the coronary arteries.

2 Related Work

The general area of 2D/3D registration can be subdivided into two distinct application types. The first type is known as projection-to-volume registration and refers to registration of images from projective 2D imaging modalities (i.e. fluoroscopy) to 3D volumes. The second type (of relevance to our work) is known as slice-to-volume registration and refers to applications where a 2D slice defined by some clipping plane in 3D space is registered to a 3D volume. Rigid slice-to-volume registration recovers the transform which places the slice into the correct position within the volume. Birkfellner et al. in [5] present the case of slice-to-volume registration with a set of common similarity metrics in application to fluoroscopic CT images and discuss its general applicability to both intra- and inter-modality registration problems. Application of slice-to-volume registration to cardiac MR data was first attempted in the work described in [6] where the slices and volumes of the same cardiac phase were successfully co-registered with a number of similarity metrics. In both cases only rigid registration methods are used, since non-rigid slice-to-volume registration in 3D can easily become an under-constrained problem.

Hennemuth et al. in [7] apply slice-to-volume registration along with other image analysis techniques to myocardium viability assessment through the use of three cardiac MR modalities: DCE-MRI, MRA and Delayed Enhancement MR (DEMR) datasets. The authors propose a solution for fusion of DCE-MRI and DEMR through the use of the high-resolution MRA dataset as a reference. In particular, DCE-MRI images are registered in 2D to the corresponding reformatted 2D slices from MRA with affine transformations excluding 3D motion; citing the results from [8] the authors in [7] claim that “3D alignment of 2D image slices is neither possible nor useful”. An example of fusion of multiple MR modalities through temporal series analysis is presented in [9] where DEMR is transformed into synthetic cine with the 4D transform derived from the analysis of cine series; this method is offered as a solution to myocardium viability assessment through the visualization of suspected scar tissue in motion. An example of 4D cine analysis presented in [10] is designed to estimate myocardium strain with physically-constrained diffeomorphic demons.

The approach for mediated spatiotemporal registration proposed in this paper is designed to fuse 2D short-axis myocardium perfusion images which were acquired at either systolic or diastolic phases of the cardiac cycle with 3D angiography volumes acquired during diastole. Contrary to the previous assertions, the approach described here shows that 3D alignment of slices is possible through the use of a 4D reference dataset to guide non-rigid registration of images acquired at distinct phases of the cardiac cycle. The evaluation results confirm that 3D alignment of perfusion slices provides better outcomes in comparison to other methods.

3 Materials and Methods

3.1 MR Imaging Protocols

The research described here relies on three types of cardiac CMR data acquired on a dedicated cardiac research scanner (1.5 Tesla Intera CV, Philips, The Netherlands). The following is a brief summary of the data; further details are given in [11]:

1. *2D DCE-MRI (stress¹ or rest) time series* (henceforward referred to as *perfusion*). A T1-weighted saturation-recovery gradient echo pulse sequence combined with SENSE is used to assess first pass myocardial perfusion in three short axis slices. The stress perfusion study commences approximately four minutes into the adenosine infusion administered to induce cardiac stress. An intravenous injection of contrast agent is administered during breath hold in end-expiration. The average field of view is 360 mm; matrix size 256×256 . Perfusion series consist of up to 60 stacks of basal, medial and apical short-axis slices of 10 mm thickness.
2. *3D MR Angiography datasets* (henceforward referred to as *angiography*). Whole heart coronary angiography is acquired using a balanced SSFP sequence and a

¹ The experiments in this work do not include perfusion stress series registration, but the spatiotemporal registration approach is equally applicable to both rest and stress series.

respiratory navigator to compensate for motion during free breathing. Timing of the diastolic coronary rest period is estimated from the four-chamber free breathing cine scan. The average field of view is 360 mm; matrix size 512×512 with up to 110 slices; slice thickness 1.79 mm.

3. *4D (3D + time) wall-motion series* (henceforward referred to as *cine series*). In clinical practice cine series are used for detecting myocardial wall motion abnormalities. Cine series are acquired with SENSE sequence as a contiguous stack encompassing both ventricles with at least 20 phases per cardiac cycle in a matrix size of 256×256 with 10–12 slices per phase (depending on left ventricular long axis length) with one to two slices acquired per breath-hold. The average field of view is 350 mm; slice thickness 10 mm.

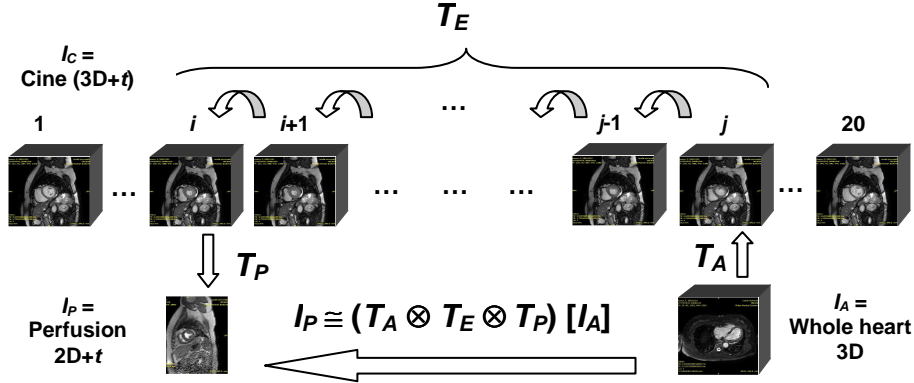
3.2 Mediated Spatiotemporal Registration

The registration method proposed here is designed to fuse 2D perfusion short-axis images of myocardium acquired at either systolic or diastolic phases of the cardiac cycle with 3D angiography volumes acquired during the phase of maximum myocardial relaxation. The method is centered around the computation of a non-rigid 3D transform to be used as a mediator for the non-rigid registration in the multi-step process attempting to link two arbitrary phases of a cardiac cycle. Prior to registration the cine series were preprocessed to correct for slice misalignment which results from the variation in breath-hold positions during series acquisition. The misalignment was corrected using the slice-to-volume registration method described in [12].

In general, image registration is described by the following equation: $T = R(I_F, I_M)$, where *fixed* image I_F is registered with *moving* image I_M to produce transform T that can be used directly to resample the moving image into the coordinate space of the fixed image. **Fig. 1** shows the stages of mediated spatiotemporal registration; the direction of the arrows indicates the direction of the derived transforms.

At the start of registration a medial or basal² perfusion slice with maximal ventricular contrast is chosen in the perfusion series; this slice is determined by the intersection of temporal intensity curves for left and right ventricles as described in [7]. The temporal phase t_p within the cine series is determined through the normalization of cardiac cycle trigger offsets which are recorded in DICOM headers; the closest value of a normalized cine trigger offset to the normalized perfusion trigger offset determines the matching cine phase t_p . Rigid slice-to-volume registration with Mutual Information (MI) metric [13] of perfusion slice I_p to the corresponding phase t_p of the cine series I_C results in a rigid transform T_p defined as follows: $T_p = R(I_p, I_C)$. The accuracy of the transform T_p is verified visually by examining the results of registration presented in a series of checkerboards (one for each cine phase) combining perfusion and phase-specific cine images; the checkerboards corresponding to cine phase t_p are characterized with the minimal discontinuities in myocardial boundaries.

² Apical, medial and basal slices are acquired at different cardiac phases due to the demands of the for DCE-MRI protocol. Apical slices were not used in this work.



* The direction of arrows indicates the direction of derived transforms.

Fig. 1. Stages of mediated spatiotemporal registration. Registration of a perfusion slice to the corresponding phase t_i in the cine dataset produces a rigid transform T_P ; registration of the whole heart angiography volume to the corresponding phase t_j in the cine dataset produces a rigid transform T_A ; non-rigid transform T_E is obtained through sequential registration of cine phases from t_i to t_j ; the total transform is composed of the transforms T_P , T_E and T_A .

Similarly, the phase match between angiography volume and cine series is found through the normalization of the cardiac cycle trigger offsets; the closest trigger value determines cine phase t_A . Rigid 3D-to-3D MI-based registration of the angiography volume I_A to the corresponding cine I_C image at phase t_A results in a rigid transform T_A defined as follows: $T_A = R(I_C, I_A)$. Again, the accuracy of the resulting transform T_A can be confirmed visually by examining the checkerboards after angiography-to-cine registration.

Given the phases of the perfusion image t_P and the angiography volume t_A the non-rigid 3D transform T_E between the t_P and t_A phases of the cine series is obtained with the composition of the transforms derived from non-rigid pair-wise registration of all adjacent phases. The composition of sequential transforms draws on the Eulerian registration framework, where the deformation is viewed as flow in time, as opposed to the deformation of an elastic material in the Lagrangian framework, where the deformation is always calculated as the transform between the first and last stages of the process [14]. Thus if a transform between two adjacent phases t_i and t_j is defined as $T_{i,j} = R(I_{C_i}, I_{C_j})$ then the composite transform T_E spanning the phases t_P and t_A is defined as follows: $T_E = T_{a,a-1} \otimes \dots \otimes T_{j,i} \otimes \dots \otimes T_{p+1,p}$, where the indices $[p, \dots, i, j, \dots, a]$ correspond to the discrete cardiac phases from t_P and t_A . In the experiments described here 3D transformations were obtained independently with two methods for non-rigid registration: MI-based registration with B-Spline transforms [15] and Demons registration [16]; both methods provided comparable outcomes. In this work we present the results for Demons registration.

It must be noted that the direction of registration at all stages is chosen in such a way so as to avoid the need for transform inversion; only direct transforms are used in the final composite transform T_M defined as follows: $T_M = T_A \otimes T_E \otimes T_P$. The

application of the transform T_M to the angiography volume I_A results in the non-rigid warping of the angiography volume into the perfusion frame of reference: $I_P \cong T_M(I_A)$. The final step involves extracting a reformatted double-oblique slice from the angiography volume at the location and orientation of the perfusion slice. When coronary arteries are defined through either manual or automatic localization (or segmentation) in the angiography volume, the composite angiography-to-perfusion transform would place the arteries into the coordinate space of the perfusion slice; segmentation of coronary arteries is not discussed in this work. The overlay of the perfusion and warped angiography images displays perfusion information in the context of the whole heart angiography volume (or vice versa, angiography in perfusion context) thus establishing the direct correspondence between perfusion defects (if present) and the closest coronary arteries. As an example output of our approach, **Fig. 2** shows (left to right) reformatted slices extracted from the original angiography volume (top and bottom) at the location and orientation of the corresponding perfusion slices, basal (top) and medial (bottom) slices from rest perfusion sequence, reformatted slices from angiography volume after the application of the final transform T_M to the angiography volume, and checkerboard overlays of perfusion and transformed angiography slices.

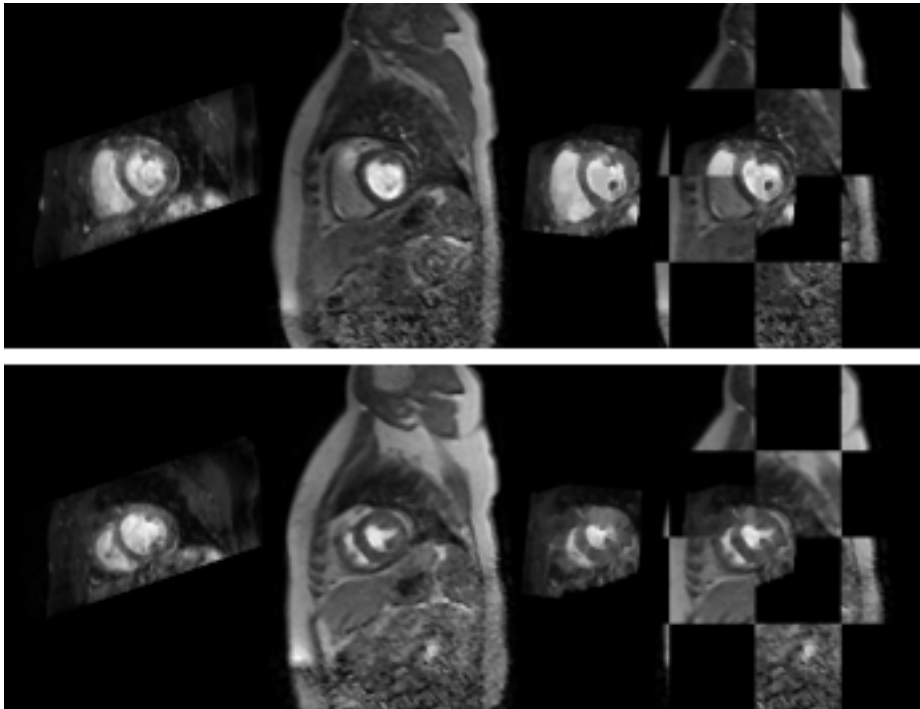


Fig. 2. Example output for registration of basal (top) and medial (bottom) perfusion slices to angiography registration: the checkerboard is composed from perfusion image (second from left) transformed angiography slice (third image).

The phase difference between perfusion and angiography images in **Fig. 2** is more striking in the case of the medial perfusion slice, because in general medial perfusion slices are acquired during systole, while angiography volume are acquired at diastole.

3.3 Evaluation Methodology

The evaluation was carried out with ten anonymized clinical datasets chosen with prior consent from the pool of data acquired for the CE-MARC study [11]; the datasets included five female and five male patients with the average age of 62 years. The registration experiments were performed with basal and medial perfusion slices with maximal ventricular contrast. The performance of our method was compared against 2D affine registration of DCE-MRI and the corresponding reformatted 2D slices from MRA without 3D alignment as described in [7].

Quantitative evaluation was carried out against ground truth with two types of manually annotated data: (1) left-ventricular (LV) endocardial, LV epicardial and right-ventricular (RV) endocardial contours for medial and basal slices with maximal myocardial contrast in both ventricles in rest perfusion data; the contours were manually drawn on QMass MR 6.2.1 from Medis Medical Imaging Systems and examined by a cardiologist, (2) manual segmentation of LV endocardial, LV epicardial and RV endocardial surfaces in whole heart angiography volumes carried out in ITK-SNAP from Penn Image Computing and Science Laboratory.

The accuracy of spatiotemporal registration was evaluated as the physical distance for each voxel from LV endocardial, LV epicardial and RV endocardial contours defined in perfusion slices to the segmented LV endocardial, LV epicardial and RV endocardial surfaces defined in angiography volumes and warped with the transform derived through mediated spatiotemporal registration. This error calculation represents the lower bound approximation of the 3D error; the true 3D error is not obtainable since the true position of the contours on the segmented LV endocardial, LV epicardial and RV endocardial surfaces at phase t_A is not known.

4 Results

The accuracy of spatiotemporal registration for medial slice is summarized in the top row of contour-to-segmentation error distance histograms in **Fig. 3**: out of the three types of contours the LV epicardial contour presents the least difficulty for our perfusion-to-angiography registration method because of its relatively large scale and simplicity of shape. Although the LV epicardial contours undergo significant expansions and contractions throughout the heart cycle, the nature of these deformations is most predictable. On the other hand the papillary muscles within the LV endocardial contour pose the most difficulty for registration because of their proximity to the endocardial surface. The RV endocardial contour is usually of a complex shape, however the deformation is successfully recovered in most cases. For comparison, the bottom row of histograms shows the contour-to-segmentation distances for 2D affine registration without 3D motion; the weaker results are

explained by insufficiency in degrees of freedom in 2D affine registration. The histograms show that the 2D affine registration has a much stronger bias in the LV endocardial contours, which can be explained by the fact that the 2D affine transform optimization is guided by the larger mass of the myocardium, while the LV endocardial contour including the LV blood pool bears less influence on the optimization process.

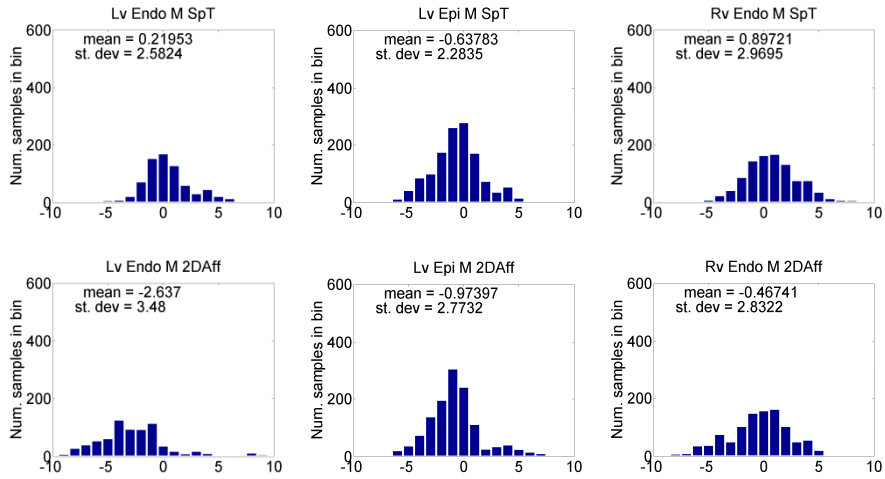


Fig. 3. Comparison of spatiotemporal registration performance (top) vs. 2D affine registration (bottom) applied to medial slices. Errors are measured as contour-to-segmentation distances (mm) for LV endocardial, LV epicardial and RV endocardial contours.

Fig. 4 shows the typical results of mediated spatiotemporal registration for one dataset; the ground truth contours (basal on top, medial below) are shown as they were defined in perfusion data; under each perfusion slice the contours are shown in the context of the transformed myocardial segmentations. As it can be seen in the example in **Fig. 2**, the shape difference to be recovered through registration is much larger for medial slices. Spatiotemporal registration, however, performs reasonably well for both basal and medial slices.

Another comparison between spatiotemporal and 2D affine registration results is shown in **Fig. 5**; Hausdorff distance and average Hausdorff distance metrics [17] measure how closely perfusion contours match the transformed myocardium segmentations; these results confirm that spatiotemporal registration is more suitable for perfusion-to-angiography registration. In the case of the medial LV endocardial and epicardial slices the t-Test indicates statistically-significant difference of the average Hausdorff distances ($P=0.001$ and $P=0.011$ respectively) between the approach presented in this work and the approach in [7].

Registration of apical slices has not been evaluated in this work, because the implementation of the method for misalignment correction in the 4D cine series needs further work; in particular the method in [18] is expected to improve the overall accuracy of our approach.

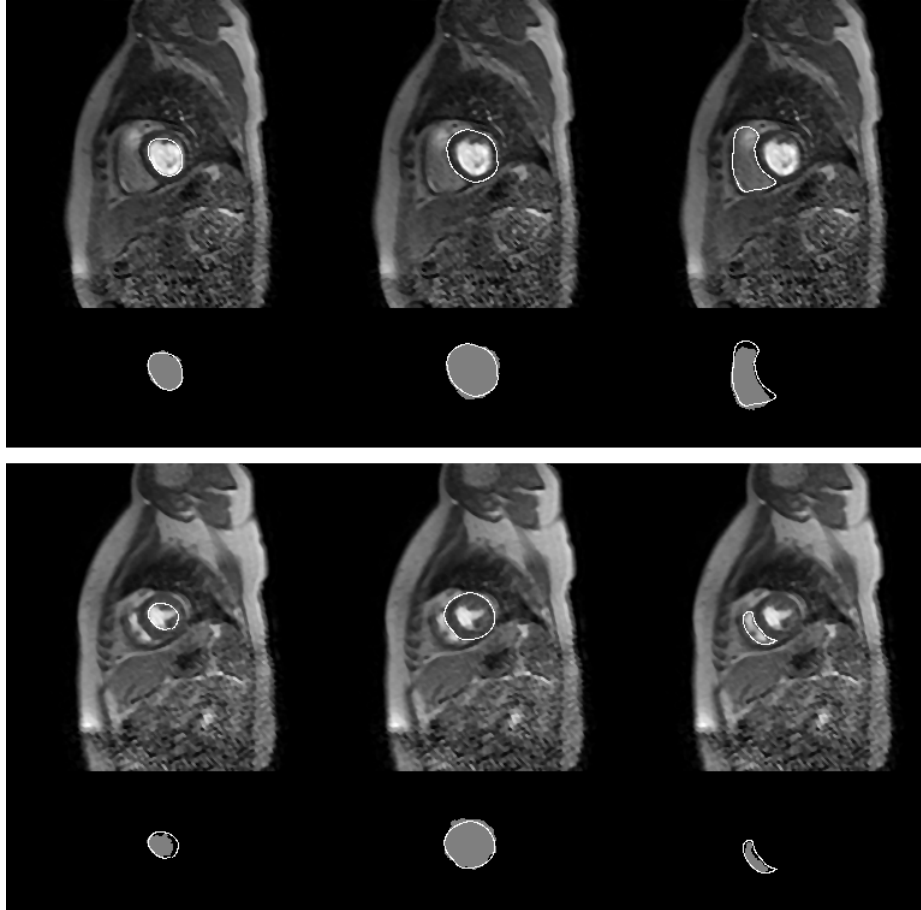


Fig. 4. LV endocardial, epicardial and RV endocardial contours in the context of basal (top) and medial (bottom) perfusion slices with respect to the transformed segmented volume.

5 Discussion

The presented approach to spatiotemporal registration has been developed as a component in a project focusing on a comprehensive analysis of CMR. The evaluation of the approach presented in this paper indicates that the method can be used for correlating angiography and perfusion datasets by recovering the perfusion-to-angiography phase difference. We intend to use the method in conjunction with coronary tree segmentation and perfusion analysis to produce patient-specific maps of coronary supply territories combined with perfusion and myocardium viability data. More generally, in combination with automatic myocardium segmentation methods in high-resolution whole-heart angiography volumes our method can be applied to the problematic task of myocardium segmentation in low-resolution perfusion data;

application of the transform spanning the phase difference between angiography and perfusion phases to automatically segmented myocardium can produce myocardium labeling in the whole perfusion series if they were initially corrected for breathing motion; to our knowledge this approach for perfusion segmentation has not been explored in research literature.

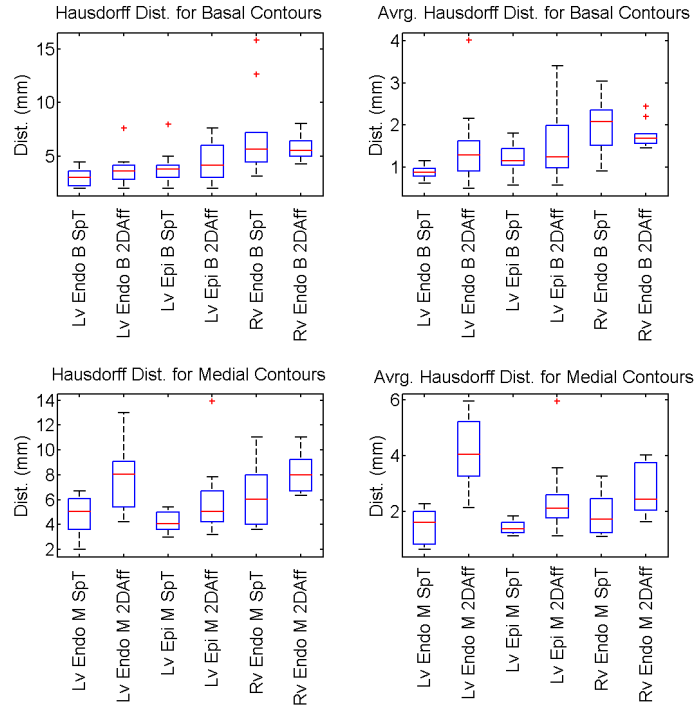


Fig. 5. Comparison of spatiotemporal (SpT) vs. 2D affine (2DAff) registration with Hausdorff distance and average Hausdorff distance for basal (previous page) and medial contours.

Although at this stage the performance of our approach on basal and medial slices presents an incremental improvement of the basic 2D affine registration, overall spatiotemporal registration has more potential for all short-axis slice locations and phase differences; in other words, while both methods demonstrate equivalent performance on “easy” data, spatiotemporal registration produces reliable results with “difficult” data. The top image in **Fig. 6** illustrates that 2D affine registration lacks in the number of degrees of freedom to recover the transform between medial perfusion slice and angiography; the images below present a case of success of 2D affine registration on a basal perfusion slice and a case of failure on a medial perfusion slice. The authors believe that although the proposed approach does not explicitly account for tissue twist that occurs during myocardial contraction and relaxation, further improvements to the approach can implicitly provide suitable accuracy for a very reliable mechanism to correlate coronary arteries to perfusion territories.

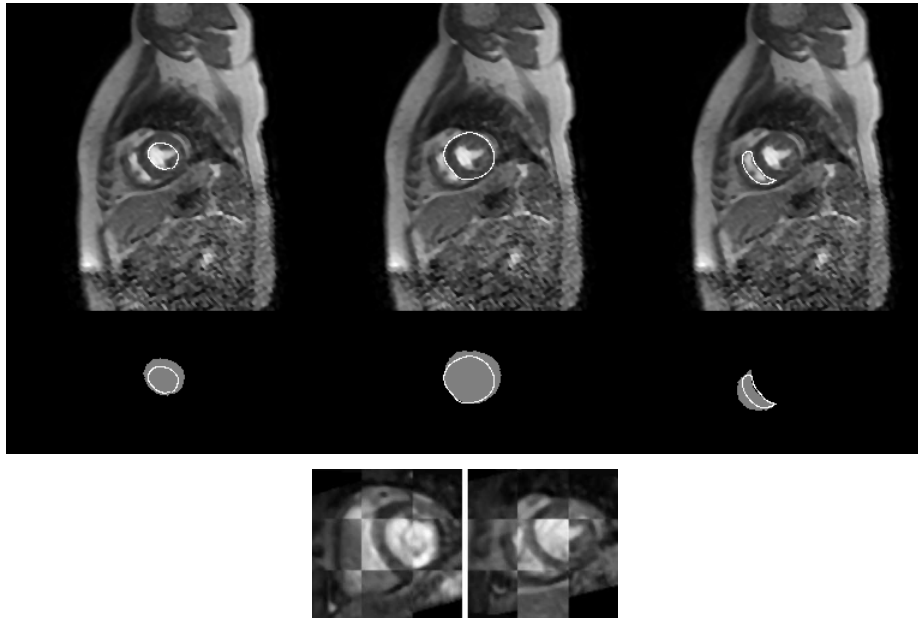


Fig. 6. Examples of successful and failed registration with 2D affine transformations. The top image demonstrates that 2D affine transform for medial perfusion slices lacks in degrees of freedom to bridge large phase-to-phase gaps. The image below shows the checkerboards from successful transform recovery for a basal slice and a failed result for a medial slice.

In conclusion, the presented approach for spatiotemporal registration of perfusion and angiography datasets improves on the previous methods. It is more general because it is capable of recovering deformations for all phases of the cardiac cycle and short-axis slice locations. It is also expected that the proposed approach will show its strength in the analysis of stress perfusion sequences

Acknowledgements: Clinical data used in this study were obtained within the CE-MARC study funded by the British Foundation Grant to Leeds CMR Unit (RG/05/004).

References

1. Plein, S., Greenwood, J.P., Ridgway, J.P., Cranny, G., Ball, S.G., Sivanathan, M.U.: Assessment of non-ST-segment elevation acute coronary syndromes with cardiac magnetic resonance imaging. *J Am Coll Cardiol* **44** (2004) 2173-2181
2. Plein, S., Radjenovic, A., Ridgway, J.P., Barmby, D., Greenwood, J.P., Ball, S.G., Sivanathan, M.U.: Coronary Artery Disease: Myocardial Perfusion MR Imaging with Sensitivity Encoding versus Conventional Angiography. *Radiology* **235** (2005) 423-430
3. Cerqueira, M.D., Weissman, N.J., Dilsizian, V., Jacobs, A.K., Kaul, S., Laskey, W.K., Pennell, D.J., Rumberger, J.A., Ryan, T.J., Verani, M.S.: Standardized Myocardial

- Segmentation and Nomenclature for Tomographic Imaging of the Heart. *Journal of Cardiovascular Magnetic Resonance* **4** (2002) 203 - 210
4. Setser, R.M., O'Donnell, T.P., Smedira, N.G., Sabik, J.F., Halliburton, S.S., Stillman, A.E., White, R.D.: Coregistered MR Imaging Myocardial Viability Maps and Multi-Detector Row CT Coronary Angiography Displays for Surgical Revascularization Planning: Initial Experience. *Radiology* **237** (2005) 465-473
 5. Birkfellner, W., Figl, M., Kettenbach, J., Hummel, J., Homolka, P., Scherthaner, R., Nau, T., Bergmann, H.: Rigid 2D/3D slice-to-volume registration and its application on fluoroscopic CT images. *Medical Physics* **34** (2007) 246-255
 6. Smolíková-Wachowiak, R., Wachowiak, M.P., Fenster, A., Drangova, M.: Registration of two-dimensional cardiac images to preprocedural three-dimensional images for interventional applications. *Journal of Magnetic Resonance Imaging* **22** (2005) 219-228
 7. Hennemuth, A., Seeger, A., Friman, O., Miller, S., Klumpp, B., Oeltze, S., Peitgen, H.O.: A Comprehensive Approach to the Analysis of Contrast Enhanced Cardiac MR Images. *Medical Imaging, IEEE Transactions on* **27** (2008) 1592-1610
 8. Rogers, W., Jr, Shapiro, E., Weiss, J., Buchalter, M., Rademakers, F., Weisfeldt, M., Zerhouni, E.: Quantification of and correction for left ventricular systolic long-axis shortening by magnetic resonance tissue tagging and slice isolation. *Circulation* **84** (1991) 721-731
 9. Gao, G., Cockshott, P.W., Martin, T.N., Foster, J.E., Elliott, A., Dargie, H., Groenning, B.A.: A novel method for viability assessment by cinematographic and late contrast enhanced MRI. In: Amir, A.A., Armando, M. (eds.), Vol. 5369. *SPIE* (2004) 700-709
 10. Mansi, T., Peyrat, J.-M., Sermesant, M., Delingette, H., Blanc, J., Boudjemline, Y., Ayache, N.: Physically-Constrained Diffeomorphic Demons for the Estimation of 3D Myocardium Strain from Cine-MRI. *Functional Imaging and Modeling of the Heart*, Vol. 5528. Springer Berlin / Heidelberg (2009) 201-210
 11. Greenwood, J., Maredia, N., Radjenovic, A., Brown, J., Nixon, J., Farrin, A., Dickinson, C., Younger, J., Ridgway, J., Sculpher, M., Ball, S., Plein, S.: Clinical evaluation of magnetic resonance imaging in coronary heart disease: The CE-MARC study. *Trials* **10** (2009) 62
 12. Chandler, A., Pinder, R., Netsch, T., Schnabel, J., Hawkes, D., Hill, D., Razavi, R.: Correction of misaligned slices in multi-slice cardiovascular magnetic resonance using slice-to-volume registration. *Journal of Cardiovascular Magnetic Resonance* **10** (2008) 13
 13. Mattes, D., Haynor, D.R., Vesselle, H., Lewellen, T.K., Eubank, W.: PET-CT image registration in the chest using free-form deformations. *Medical Imaging, IEEE Transactions on* **22** (2003) 120-128
 14. Avants, B., Sundaram, T., Duda, J.T., Gee, J.C., Ng, L.: Non-rigid image registration. In: Yoo, T.S. (ed.): *Insight into Images: Principles and Practice for Segmentation, Registration, and Image Analysis*. AK Peters (2004) 307-348
 15. Rueckert, D., Sonoda, L.I., Hayes, C., Hill, D.L.G., Leach, M.O., Hawkes, D.J.: Nonrigid registration using free-form deformations: application to breast MR images. *Medical Imaging, IEEE Transactions on* **18** (1999) 712-721
 16. Thirion, J.-P.: Non-Rigid Matching Using Demons. *Computer Vision and Pattern Recognition. IEEE Computer Society* (1996) 245-251
 17. Huttenlocher, D.P., Klanderman, G.A., Rucklidge, W.A.: Comparing Images Using the Hausdorff Distance. *IEEE Transactions on Pattern Analysis and Machine Intelligence* **15** (1993) 850-863
 18. Lötjönen, J., Pollari, M., Kivistö, S., Lauerma, K.: Correction of Movement Artifacts from 4-D Cardiac Short- and Long-Axis MR Data. *Medical Image Computing and Computer-Assisted Intervention – MICCAI 2004* (2004) 405-412